(This is a sample cover image for this issue. The actual cover is not yet available at this time.)

Journal of Luminescence 132 (2012) 1957–1963

Contents lists available at SciVerse ScienceDirect

Journal of Luminescence

journal homepage: www.elsevier.com/locate/jlumin

Design and optimization of light emitting devices based on CdTe-QD as an emissive layer

Sh.G. El-sherbiny [b,c], S. Wageh [a,*], S.M. Elhalafawy [b], A.A. Sharshar [b]

[a] Physics & Engineering Mathematics Department, Faculty of Electronic Engineering, Menufiya University, Menouf 32952, Egypt
[b] Department of Electronics and Electrical Comm., Faculty of Electronics Eng. Menufiya University, Menouf 32952, Egypt
[c] Electrical Engineering Department, Faculty of Engineering, Kafrelsheikh University, Kafr el-Sheikh, Egypt

ARTICLE INFO

Article history:
Received 11 October 2011
Received in revised form
21 February 2012
Accepted 2 March 2012
Available online 13 March 2012

Keywords:
Microcavity light emitting devices
Quantum dots
CdTe

ABSTRACT

We present a detailed design method of quantum dot-organic light emitting devices (QD-OLED) based on microcavity model. CdTe quantum dot is used as an emissive layer for blue, green and red emissions. We have simulated the internal photoluminescence emissions of the quantum dot layer by Gaussian function based on the published experimental results. Using these simulated internal photoluminescence emissions for different quantum dot sizes we have calculated the output emissions intensities of blue, green and red lights. We have investigated the effect of changing the device geometry on the emission intensity. We found that the emission intensity is highly depends on the device geometry. On the other hand, we found that the optimizations of the device structure are different for different emissions colors.

1. Introduction

Recently, optoelectronic devices have become essential elements in optoelectronics based hardware technology in the area ranging from communication systems to consumer electronics [1]. Light emitting diode (LED) is considered as one of the most important optoelectronic devices. During the last five decades, LEDs have undergone a significant development, the first LEDs emitting in the visible wave length region were based on GaAsP compound semiconductor with external efficiency of only 0.2%. Since that time, a lot of developments have been introduced to improve the performance of such inorganic LEDs [2].

For certain device applications, semiconducting polymers can replace inorganic semiconductors at low cost because they are more easily processed, one example of these applications, is the development of organic light emitting diodes(OLEDs) for full-color light emitting displays[3]. Organic LEDs have sufficient brightness, range of color and operating life times to make them a possible alternative to liquid crystal based flat panel displays [4]. Recently, a hybrid device of an OLED incorporating nanocrystal (NC) quantum dots (QD) has been suggested as a new form for solid state lighting [5,6]. This hybrid device has the advantages of exhibiting high brightness, narrow spectral full width at half maximum (FWHM) and QD size dependence of the emission peak of the photoluminescence. The excellent size dependent, bright and narrow photoemission of colloidal semiconductor cadmium nanocrystals, such as CdS, CdSe and CdTe, combined with the flexibility in process ability enables them to be used in solution processed hybrid of organic and inorganic LEDs [7].

Although, CdSe is frequently used in LEDs, CdTe NCs have an advantage in terms of band alignment which in turn provides a significant reduction of the barrier for hole injection compared to CdSe [7]. Since the device modeling has become a powerful tool as it avoids tedious experiments and offers exploration into wide range of critical microscopic behaviors, this paper concerns with the design and optimization of an organic LED based on CdTe NCs as an emissive layer using microcavity modeling. Up to now optical studies on device simulation and design on light emitting devices based on quantum dots are very rare [8–12]. In this work, we have designed three devices based on CdTe quantum dot as emissive layer for blue, green and red light emissions. Also, we have investigated the effect of device geometry and cavity length on the emission intensity.

This paper organized as follows; Description of the device structure and the microcavity model, the design method and simulation parameters, the results and discussions and finally, the conclusions are drawn.

2. Device structure and microcavity modeling of QD-OLED

A schematic diagram of a typical microcavity QD-OLED with a multilayer structure is shown in Fig. 1. Where Al and Ag represent the upper and lower metallic mirrors, respectively. We have used here metallic mirrors instead of high-performance dielectric

* Corresponding author. Tel.: +20 103592706; fax: +20 483660716.
E-mail address: wageh1@yahoo.com (S. Wageh).

0022-2313/$ - see front matter © 2012 Elsevier B.V. All rights reserved.
doi:10.1016/j.jlumin.2012.03.006

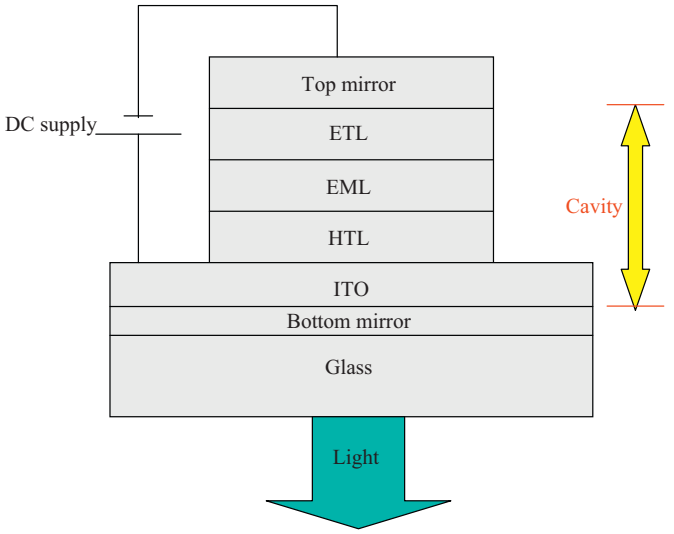

Fig. 1. The schematic of microcavity light emitting device used in calculations of ITO/TPD/CdTe (quantum dots)/ Alq_3/AL, with Ag as bottom reflecting mirror.

mirrors, to maintain fabrication simplicity (only one layer must be deposited) and hence, suitability for applications in microsystems because of its small size. In addition, the metallic mirrors can be applied over a wide spectral range of frequency, because of the high reflectivity of silver and aluminum in the visible range [13]. Our future work is the comparison of the performance of the devices based on metallic and dielectric mirrors. ETL, EML, HTL refer to the electron transporting layer, emissive layer and hole transporting layer, respectively. In case of QD-OLED, the emissive layer consists of nanocrystal quantum dots of a semiconducting material. We have used here the same method that was used for simulation of the microcavity OLED [14] to design and simulate the emission of QD-OLED. The external emission spectrum of the microcavity device can be calculated by:

$$I_{cav.}(\lambda)=\frac{1}{N}\sum_{i=1}^{N}\frac{(1-R_L)(1+R_U+2\sqrt{R_U}\cos(4\pi z_i\cos\theta_{in}/\lambda+|\varphi_U|))}{1+R_UR_L-2\sqrt{R_UR_L}\cos(4\pi L\cos\theta_{in}/\lambda+|\varphi_U|+|\varphi_L|)}I_{in}(\lambda) \quad (1)$$

where, λ is the wave length, R_U and R_L are the reflectivity of the upper and lower interfaces of the cavity (metallic mirrors), respectively. z_i is the optical distance of the emitting dipoles to the metal mirror, ϕ_U and ϕ_L are the wave length dependent phase changes upon reflection from upper and lower mirrors, respectively. $I_{in}(\lambda)$ is the free space spontaneous emission of the emissive layer. L is the optical thickness of the cavity ($L=\sum T_i n_i(\lambda)$). T_i and n_i are the physical thickness and refractive index of the ith layer, respectively.

3. Materials and optical parameters used in simulation model

The device considered consists of Al and Ag as metallic mirrors, Alq_3 as electron transporting layer, TPD as hole transporting layer and CdTe quantum dots as an emissive layer. In this section we discuss the optical parameters for each layer which have been used in simulation model.

3.1. Spontaneous emission ($I_{in}(\lambda)$)

The spontaneous photoluminescence emissions of CdTe quantum dots have been simulated using Gaussian distribution function.

First, we have collected from the published experimental results the data which relate the size of the quantum dots and the position of the emission peaks [9]. Then, through fitting the experimental results we have found the fitting equation that relates the size of the quantum dot and the position of emission peak wave length. The obtained fitting equation is:

$$P=11.108d^2+39.439d+321.11 \quad (2)$$

where d is the QD diameter. Fig. 2(a) shows the agreement between the experimental data and the fitted curve for the relation between the emission peak position and quantum dot size.

Then, using Eq. (2) we can simulate the spontaneous emission as follows:

$$I_{in}(\lambda)=\exp(-(\lambda-P)^2/2c^2) \quad (3)$$

where P is the position center of the peak and c is a factor related to the full width at half maximum (FWHM) according to $FWHM=2\sqrt{2\ln 2}c$. We have applied 35 nm for the FWHM of CdTe QD emission [12]. Fig. 2(b) represents the simulated photoluminescence emissions for different sizes of CdTe quantum dots.

3.2. Refractive indices of the materials used

The refractive index of the emissive layer which in our case is CdTe QDs, was determined using the equation developed in literature

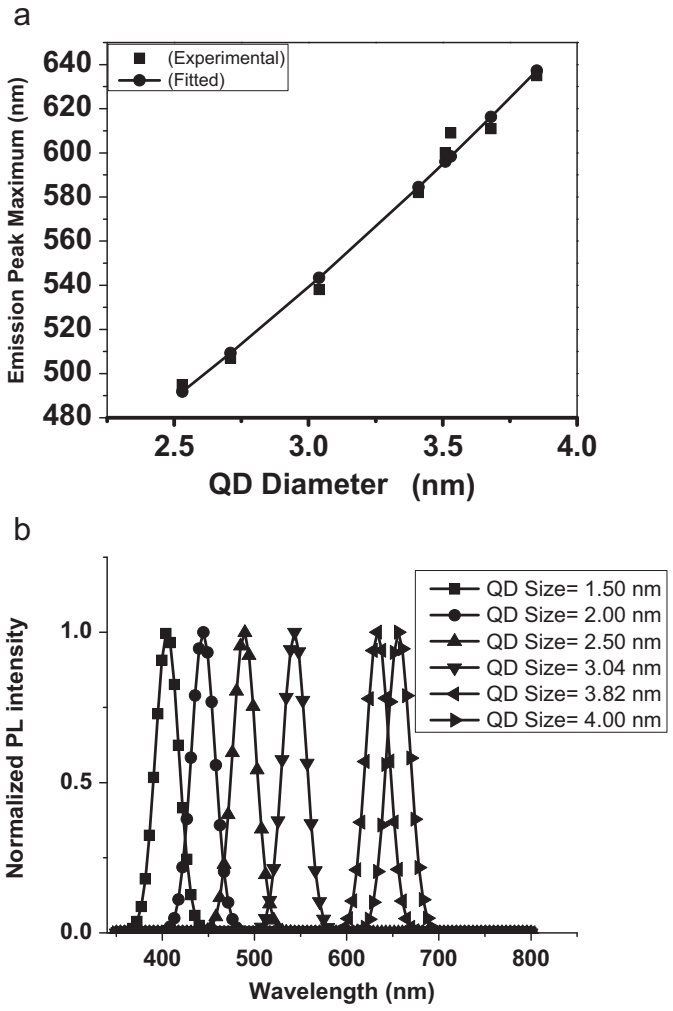

Fig. 2. (a) Position of photoluminescence (PL) emission peak maximum versus QD diameter, (b) Simulated photoluminescence emission profiles of CdTe for 1.5, 2.0, 3.04, 3.82 and 4.0 nm QD sizes.

Table 1
Refractive indices of materials used for building the device of the three emission colors blue, green and red.

Material	Refractive index at λ=445 nm	Refractive index at λ=543 nm	Refractive index at λ=633 nm
Alq_3	1.8111	1.753	1.74
TPD	1.822	1.753	1.74
ITO	2.4+0.01i	2+0.01i	1.94
Al	0.61564+5.39411i	0.928+6.6i	1.374+7.62i
Ag	0.1553+2.42i	0.128+3.282i	0.135+3.988i

which relates the refractive index with the size of QD [15]:

$$n=\left[1+(\varepsilon_{\text{bulk}}-1)/(1+0.75/d)^{1.2}\right]^{1/2}$$

where $\varepsilon_{\text{bulk}}$ is the dielectric constant of the bulk material and d is the average diameter of the QD in nanometer. In our calculation we take the value of refractive index for bulk CdTe to be 2.69 [16] and then the dielectric constant is calculated as the square of the refractive index [17]. This value of dielectric constant will be approximately reasonable if we disperse the quantum dots in a high dielectric constant solvent such as chloroform or tetrahydrofuran.

The frequency-dependent refractive indices of Al and Ag are calculated using the Drude formula [18].The refractive indices of Alq_3 and TPD at different wavelengths were obtained from the measured spectrum of optical parameters found in [19]. It was found that, the refractive indices of Alq_3 and TPD have very small difference in the visible range. As we interested for the study of the devices emit blue, green and red emissions, we have determined the refractive indices of different materials at 445, 543 and 633 nm wavelengths which are listed in Table 1.

4. Design and simulation

We have simulated the emitted radiation of CdTe QD-OLED microcavity device. We have applied the following steps to compute the emission, in case of normal incidence, for different wavelengths and different device geometries:

First, based on Eq. (1) the resonance of the cavity for the normal incidence occurs at:

$$\sum\frac{4\pi}{\lambda}T_i n_i(\lambda)+|\phi_U(\theta,\lambda)|+|\phi_L(\theta,\lambda)|=2m\pi \quad (4)$$

i. Determine the resonance of the required emission peak wavelength (λ_{res}) by applying resonance formula (Eq. (4)), then estimate the compatible QD size matching this wavelength using Eq. (2). Then, simulate the internal emission profile by applying Eq. (3).
ii. Estimate the reflectivity and phase changes upon reflections from upper and lower metallic mirrors.
iii. Estimate the optical thickness (L_{op}) of the materials consisting the device at normal incidence and resonance wavelength (λ_{res}) using Eq. (4).
iv. Estimate the physical thickness (L_{ph}) of the materials consisting the device through $L_{\text{op}}=n_{\text{cav}}.L_{\text{ph}}$.
v. Adopting the geometry of each device by applying the following relation between emission layer thickness, ITO layer thickness and total optical thickness:

$$L_{\text{Op}}=n_{\text{ITO}}.T_{\text{ITO}}+n_{\text{EM}}.T_{\text{EM}}+n.(L_{\text{ph}}-T_{\text{ITO}}-T_{\text{EM}}) \quad (5)$$

where n is the refractive index of HTL and ETL.

Finally, based on the previous steps, the thickness of each layer can be estimated and optimized for maximum luminescence intensity.

5. Results and discussion

We have investigated the emission spectra of three devices based on CdTe QDs as an emissive layer, for emissions at 445, 543 and 633 nm which correspond to blue, green and red emissions, respectively.

We have investigated the first mode (m=1) of blue, green and red emissions for the device consists of Glass/Ag/ITO/TBD/ Alq_3/ Al. Table 1 summarizes the calculated QD diameter, optical thickness of the materials inside the cavity and the physical thickness for the devices emit blue, green and red emissions colors with (m=1). The calculated physical thicknesses matching the resonance for blue, green and red emissions are 73, 85 and 99 nm, respectively. We have studied the relation between ITO thickness and the thickness of the emissive layer (with constant value of the sum of HTL and ETL) by applying Eq. (5). This study gives us how to vary the device geometry with conserving the resonance. Fig. 3 shows the relation between the ITO thickness against emission layer thickness for the first mode of resonance (m=1) of blue green and red emissions. Here, each value of EML thickness and ITO thickness is restricted to a certain value that can fix the resonance at the required wave length. According to the relation between the ITO thicknesses against emission layer thickness we have restricted the EML layer thickness to 20 nm and varying the thickness of ITO layer. The values of ITO thickness are 22, 25 and 44 nm for blue, green and red emissions, respectively. Then for each value of ITO layer thickness we have optimized the devices through changing the HTL and ETL layer thicknesses. Figs. 4–6 show the blue, green and red emissions with different HTL and EML layers thicknesses. Clearly, with increasing the HTL thickness and decreasing the ETL layer thickness the emission intensity increases for the blue, green and red emissions. We attributed this result to the change in the distance between the recombination zones (i.e., emitting centers) to the cathode where the reflection is most significant. This means that the change of the distance between the emissions centers and the cathode plays an important role in optimizing the optical density. It is worth to mention that the intensity of the red emission is

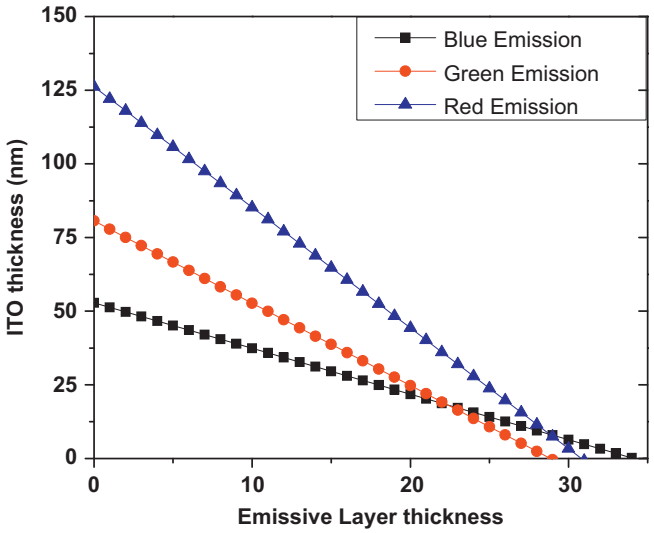

Fig. 3. Relation between ITO layer thickness and emissive layer thickness for blue, green and red emissions for the devices designed for resonance with first mode m=1.

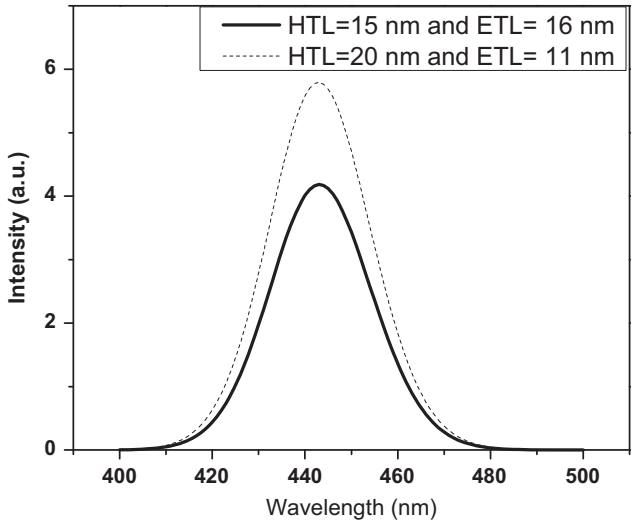

Fig. 4. Variation of emission intensity for different HTL thicknesses in case of the first resonance mode of blue emission with EML=20 nm and ITO=22 nm.

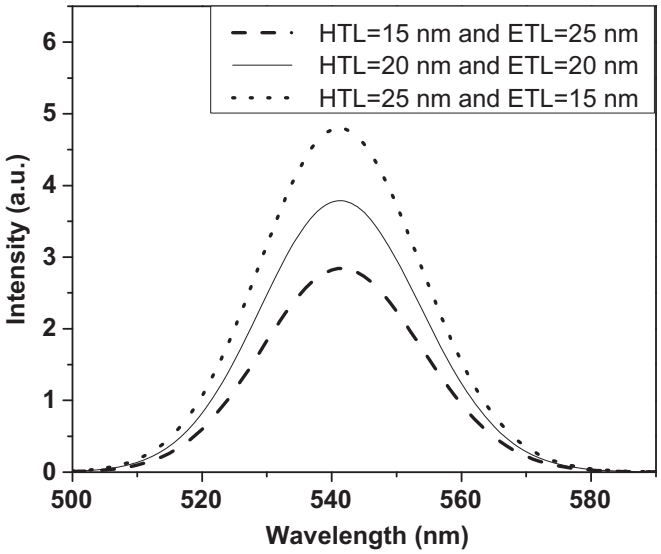

Fig. 5. Variation of intensity for different HTL thicknesses in case of the first resonance mode of green emission with thicknesses of EML=20 nm and ITO=25 nm.

high in comparison with blue and green emissions devices. We ascribed this result to the variation in wavelength which results in variation in refractive index of the cavity and hence the magnitude and phase of reflection coefficients which leads to the variation of intensity. We should bear in mind that, the change in ITO layer thickness will affect on the resistivity of ITO layer [20] and consequently affect on the device performance. So, to completely optimize the emission of devices we should compromise the study of optical and electrical characteristics which will be the future work.

Also we have investigated the second mode of resonance ($m=2$) for blue, green and red emissions for the device consists of Glass/Ag/ITO/TBD/ Alq_3/Al. Table 2 summarizes the calculated QD diameter, optical thickness of the materials inside the cavity and the physical thickness for the devices emit blue, green and red emissions colors with ($m=2$).

In this case there is a chance to highly increase the physical thickness relative the first resonance mode with ($m=1$). To decide

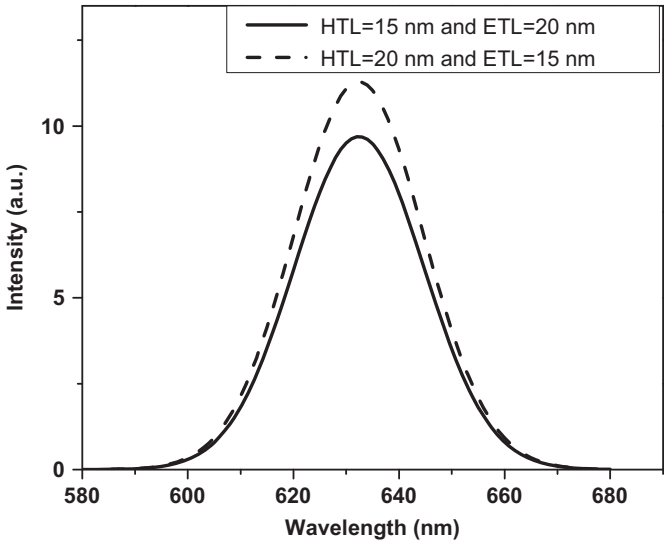

Fig. 6. Variation of intensity for different HTL thicknesses in case of the first resonance mode of red emission with thicknesses of EML=20 nm and ITO=44 nm.

Table 2
Optical thickness and physical thickness matches first resonance mode ($m=1$) of the cavity for different emissions wavelengths, which correspond to different QD sizes.

Wavelength (nm)	445	543	633
QD diameter in (nm)	2	3.04	3.82
Optical thickness (nm)	149.3	170	197
Physical thickness (nm)	73.5	85	99

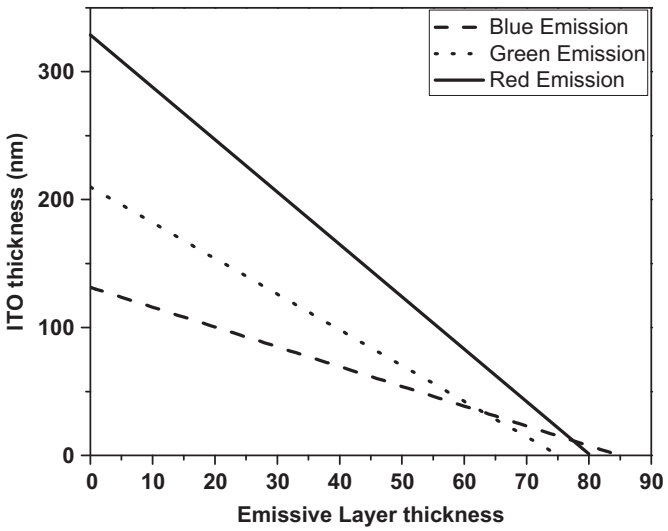

Fig. 7. Relation between ITO layer thickness and emissive layer thickness for blue, green and red emissions for the devices designed for resonance with second mode $m=2$.

the required physical thickness of both HTL and ETL layers which corresponding to maximum emission intensity for blue, green and red emissions. Also, we have studied for second resonance mode the relation between ITO thickness and the thickness of the emissive layer (with constant value of the sum of HTL and ETL) to investigate the most possible variations of the device geometry.

Fig. 7 shows the relation between the ITO thickness and emission layer thickness for the second mode of resonance of blue, green and red emissions. Clearly, for each value of EML thickness, the ITO thickness is restricted to a certain value that can fix the resonance at the required wave length. For example the device designed for red emission (at 633 nm), we have found that the less value for EML thickness is 35 nm, and this is because EML with thickness smaller than this value restricts ITO thickness to a value very close to the total physical thickness of the device and consequently unreasonable thickness for ETL and HTL.

Table 3
Optical thickness and physical thickness matches the second resonance mode ($m=2$) of the cavity for different emissions wavelengths, which correspond to different QD sizes.

Wavelength (nm)	445	543	633
QD diameter in (nm)	2	3.04	3.82
Optical thickness (nm)	371	442	514
Physical thickness (nm)	183	221	258

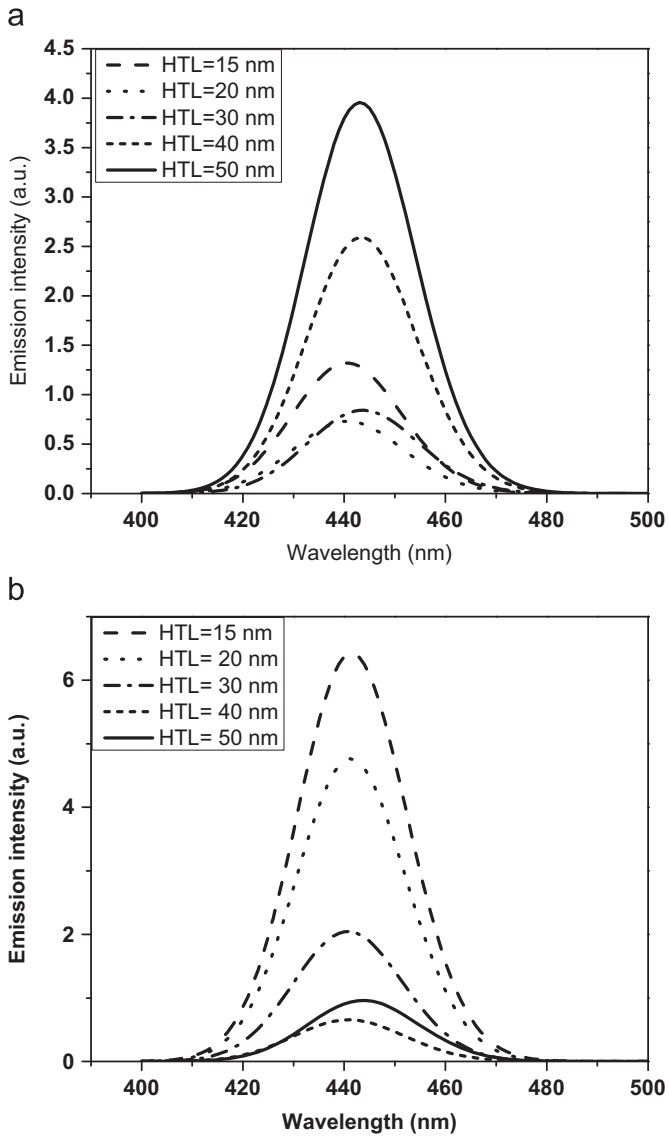

Fig. 8. EL intensity with changing HTL thickness for second resonance mode of blue emission: (a) EML thickness of 20 nm, (b) EML thickness of 30 nm.

Table 3 Based on the relation between ITO thickness and the thickness of the emissive layer with a constant value of the sum of HTL and ETL we have investigated the effect of varying the device geometry through the thickness of each layer on the emission spectra. Here, for each pair of ITO and EML layers thicknesses there is a value of the sum of (HTL+ETL) and hence, increasing HTL thickness means decreasing ETL thickness and vice versa.

Figs. 8(a) and (b) show the effect of increasing the HTL thickness on the expense of ETL thickness on the luminescence emission intensity with thicknesses of EML=20 and 30 nm, respectively. It was noted that, for the device designed with EML=20 nm, the increasing in HTL thickness up to 30 nm leads to a decrease of emission intensity. By further increasing of HTL thickness the emission intensity highly increases. While for the device designed with EML=30 nm the emission intensity continuously decreasing with increasing HTL thickness up to 40 nm and slightly increased for the HTL=50 nm. These results indicate that upon the variation of HTL and ETL thicknesses the device performance is highly dependent on the thickness of EML layer. So, we decided to investigate the effect of varying EML thickness on the emission intensity for the devices having various HTL thicknesses. Fig. 9 shows the effect of changing EML thickness on the emission intensity with varying HTL thicknesses. Clearly, for the thicknesses of HTL equal 15 and 20 nm, the emission peak intensity increases with increasing EML thickness. While for the thicknesses of HTL equal 30 and 40 nm, the emission peak intensity first decreases with increasing EML thickness up to 30 nm. But for the higher values more than 30 nm of EML thickness the emission intensity continuously increase with increasing EML thickness. By changing EML and HTL thickness we have two effects on the emission intensity (1) the increase of EML thickness on the expense on ITO layer (this effect is very small because the difference between the refractive index of the quantum dot and the ITO is very small), (2) the change of the optical distance of the emitting center to the metal mirror which improve the alignment with antinode position of the field. We can consider the second effect is predominant reason for the increase of the emission intensity with increasing the EML layer thickness for the devices based on thicker EML layer.

Figs. 10 and 11 show the effect of increasing HTL layer thickness on the emission intensity of the green light for various EML layer thicknesses. Clearly, the emission intensity decreases with increasing HTL layer thickness from 20 to 30 nm, then

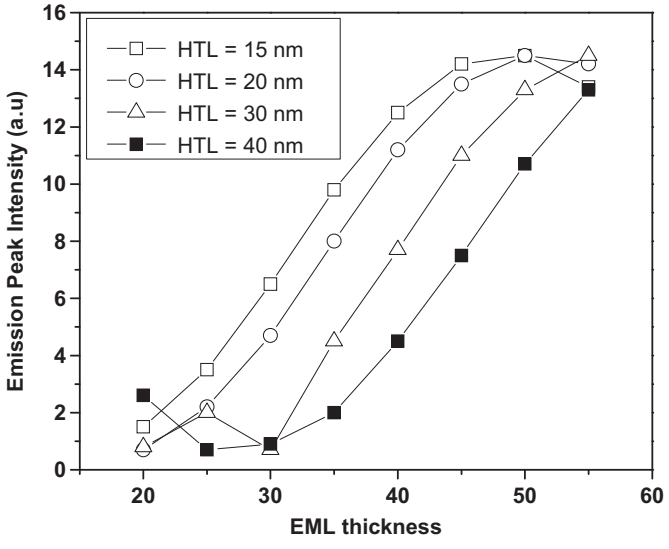

Fig. 9. Emission peak intensity for the second resonance mode of blue emission versus EML thickness with different HTL thickness.

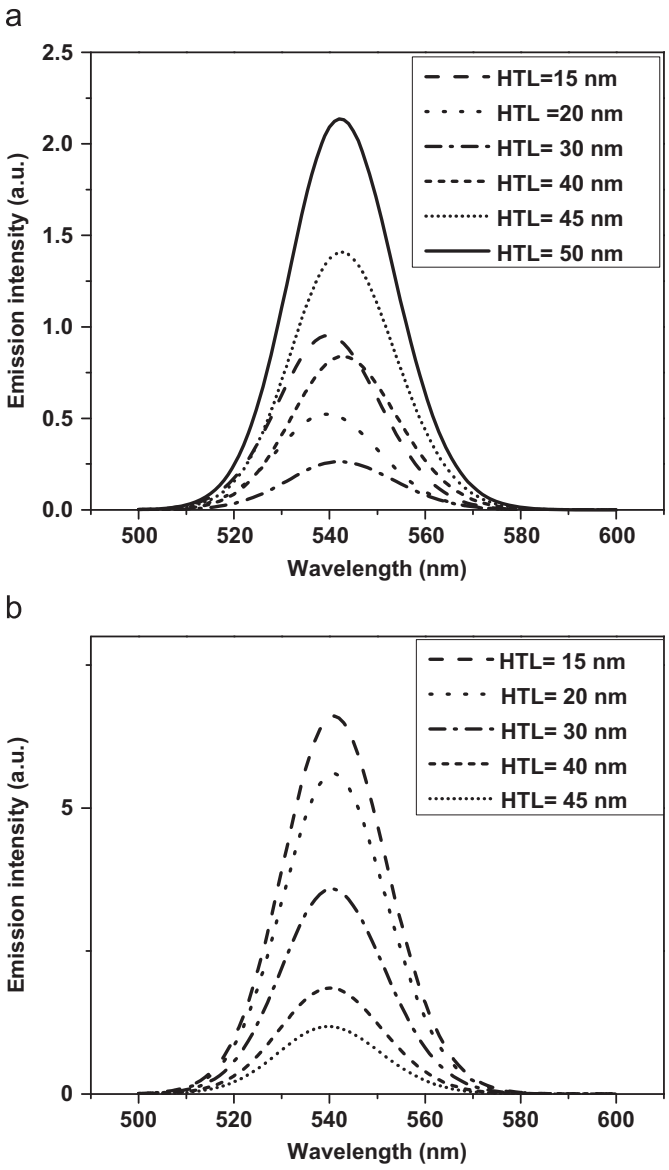

Fig. 10. EL intensity with changing HTL thickness for second resonance mode of green emission (a) EML thickness of 30 nm, (b) EML thickness of 40 nm.

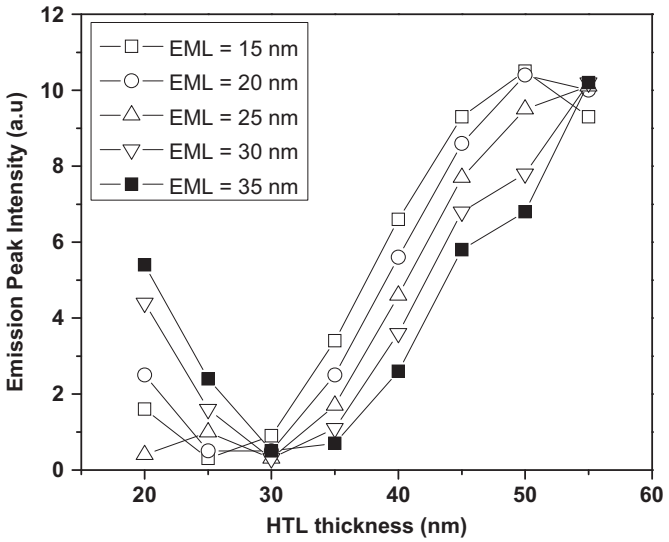

Fig. 11. Variation in the output emission intensity of second resonance mode of green emission against HTL thickness for various EML layer thicknesses.

emission intensity starts to increase with increasing the HTL layer thickness up to 55 nm. On the other hand, the effect of increasing the EML layer thickness leads to a decrease in emission intensity which is opposite in trend relative to design of blue emission. Here, the design of the cavity length for green is thicker than that one for blue light emission device due to the increase of QD refractive index. This longer cavity length will affect on the position of alignment with antinode of the field. Also, the reflectivity of the cathode for the green light is different from the blue light which will also affect on the resonance of the device.

Fig. 12(a) and (b) show the effect of changing the HTL layer thickness for device designed for red light emission with EML layer thicknesses 50 and 60 nm, respectively. Here, we selected thicker EML layer thickness due to longer cavity length relative to green and blue emissions. It is noted that the increase of HTL layer thickness leads to decrease of the emission intensity. On the other hand, the emission intensity of red color is relatively higher than the emission intensities of green and blue emissions. We attributed this increase in intensity to the increase of reflectivity of cathode to red light relative to the reflectivity to green and blue light.

It is worth to mention that, our calculations for the devices designed with EML layer with 40 nm or more the position of the emissions peaks are not have noticeable change with increasing the HTL layer thickness. While the devices designed with EML layer thickness equal 30 nm or less there is a nonsystemically change in the position of the emission peaks with increasing the thickness of HTL layer on the expense of ETL layer. In the case of the thicker EML layer, the change in HTL layer thickness has very small effect on the optical length of cavity that is because the EML layer has high dielectric constant relative to HTL and ETl layers. In addition, the difference in the dielectric constants between ETL and HTL is very small. While for the case of thin EML layer the change in HTL layer thickness will give a noticeable change in optical length of the cavity. Consequently, the change in the optical length of the cavity affect on the resonance of the emission. So, to keep the resonance of the cavity the emission wavelength should change in this case.

We have compared our results with available systematic study of the noncavity light emitting devices by Mattoussi et al. [21]. The work published by Mattoussi et al. is a systematic study of light emitting devices based on CdSe nanocrystals while our work based on CdTe nanocrystals. So, we have adopted the difference in the peak positions according to the difference of the bulk band gaps of the two materials. We found that the difference between the position of the emission band of our work and the experimental work by about 6%. We attributed this difference to the difference in the structures of the two devices. On the other hand, we have found a good improvement in the sharpening of emission peak with application of the cavity on the devices. The half width of emission peak decreased by about 10 nm relative to the spontaneous photo-luminesnce emission and the experimental work by Mattoussi et al. Also, we compared our work with the published theoretical and experimental work about organic light emitting devices and we found in general, the results for optical properties obtained from our design methodology agree well with the general behavior of the obtained results found in references [22–23].

Finally, this work have directed to the simulations of the devices which emit the three primary colors blue, green and red emissions. Our future work we will consider the simulation of the design that produces white light based on the obtained results in this work.

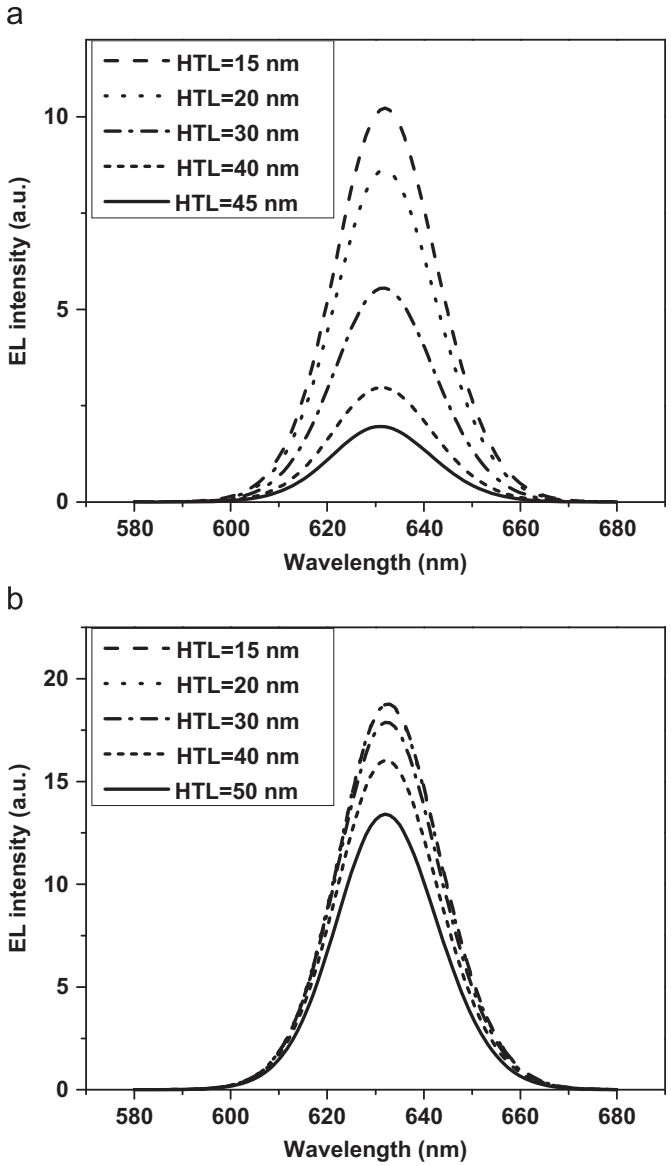

Fig. 12. EL intensity with changing HTL thickness for second resonance mode of red emission (a) EML thickness of 50 nm, (b) EML thickness of 60 nm.

6. Conclusion

A detailed design method for microcavity QD-OLED was introduced through this paper. Three LEDs for blue, green and red emissions were designed and simulated. From the simulated results, QD-OLED can be optimized by changing the device geometry through varying the thicknesses of the layers which consisting the device. We found that the optimizations for the device structures are different for different colors. On the other hand, we have compared our results with the experimental work and found fairly good agreement between our results and experimental one.

References

[1] El-Sayed A.M. Hasaneen, Mohamed Moness, M.S. Yaseen, J. Commun. Comput. 6 (10) (2009) 70–75. Serial No.59.
[2] Klaus Mullen, Ullrich Scherf, Organic Light Emitting Devices. Synthesis, Properties and Applications, Wiley-VCH Verlag GmbH& Co.KGaA, Weinheim, 2006.
[3] Nir Tessler, Vlad Medvedev, Miri Kazes, Shihai Kan, Uri Banin, Science 295 (5559) (2002) 1506–1508.
[4] Zilan Shen, Paul E. Burrows, Vladimir Bulovic, Stephen R. Forrest, Mark E. Thompson, Science 276 (5321) (1997) 2009–2011.
[5] Polina O. Anikeeva, Jonathan E. Halpert, Moungi G. Bawendi, Vladimir Bulović, Nano Lett. 7 (8) (2007) 2196–2200.
[6] Polina O. Anikeeva, Jonathan E. Halpert, Moungi G. Bawendi, Vladimir Bulović, Nano Lett. 9 (7) (2009) 2532–2536.
[7] Patrick T K Chin, Jan W Stouwdam, Svetlana S van Bavel, René A J Janssen, Nanotechnology 19 (20) (2008) 205602. (1-8).
[8] K. Kohary, V.M. Burlakov, D.G. Pettifor, J. Optoelectron. Adv. Mater. 9 (1) (2007) 18–23.
[9] A.E. Morra, S. Wageh, A.A. El-Azm, Opt. Quantum Electron. 42 (2011) 285–296.
[10] A.E. Farghal, S. Wageh, A.A. El-Azm, Prog. Electromagnet. Res. C 19 (47) (2011).
[11] Ahmed E. Farghal, S. Wageh, A.A. El-Azm, Opt. Quantum Electron. 42 (2010) 263.
[12] E. Farghal, S. Wageh, A.A. El-Azm, J. Comput. Electron. 10 (2011) 414–423.
[13] H.A. Macleod, Thin-Film Optical Filters, 2nd edn, Adam Hilger Ltd, 1986.
[14] Chien-Cheng Daniel Poitras, Kuo, Christophe Py, Opt. Express 16 (11) (2008) 8003–8015.
[15] Chenli Gan, Yanpeng Zhang, S.W. Liu, Yunjun Wang, Min Xiao, Opt. Mater. 30 (9) (2008) 1440–1445.
[16] D.T.F. Marple, J. Appl. Phys. 35 (1964) 539–542.
[17] Mark Fox, Opt. Prop. Sol., Oxford University Press, 2001.
[18] A.K. Sharma1, G.J. Mohr, New J. Phys. 10 (2) (2008) 023039. (1-12), (2008).
[19] Francis G Celii, Tracy B Harton, O. Faye Phillips, J. Electron. Mater. 26 (4) (1997) 366–371. IS.
[20] S.H. Mohamed, F.M. El-Hossary, G.A. Gamal, M.M. Kahlid, Acta Phys. Pol. A 115 (3) (2009) 704–708.
[21] Hedi Mattoussi, Leonard H. Radzilowski, Bashir O. Dabbousi, Edwin L. Thomas, Moungi G. Bawendi, Michael F. Rubner, J. Appl. Phys. 83 (1998) 7965–7974.
[22] Beat Ruhstaller, Tilman Beierlein, Heike Riel, Siegfried Karg, J. Campbell Scott, Walter Riess, IEEE J. Sel. Top. Quantum Electron. 9 (3) (2003) 723–731.
[23] Shu-Hsuan Chang, Yung-Cheng Chang, Cheng-Hong Yang, Jun-Rong Chen, Yen-Kuang Kuo, Proc. SPIE 6134 (2006) 187–196.